Guard cell endomembrane Ca^{2+}-ATPases underpin a 'carbon memory' of photosynthetic assimilation that impacts on water use efficiency

Mareike Jezek[1,7], Fernanda A.L. Silva-Alvim[1,7], Adrian Hills[1,7], Naomi Donald[1], Maryam Rahmati Ishka[4], Jessica Shadbolt[1], Bingqing He[2], Tracy Lawson[5], Jeffrey F. Harper[4], Yizhou Wang[2,8], Virgilio L. Lew[3,8], and Michael R. Blatt[1,2,6,8 *]

[1]Laboratory of Plant Physiology and Biophysics, University of Glasgow, Bower Building, Glasgow G12 8QQ UK

[2]Institute of Crop Science, College of Agriculture and Biotechnology, Zijingang Campus, Zhejiang University, Hangzhou, China

[3]Physiological Laboratory, University of Cambridge, Downing Street, Cambridge CB2 3EG UK

[4]Department of Biochemistry and Molecular Biology, University of Nevada, Reno, Nevada 89557 USA

[5] School of Life Sciences, University of Essex, Wivenhoe Park, Colchester CO4 3SQ

[6]Author for manuscript correspondence and post-publication queries (Michael.Blatt@glasgow.ac.uk; +44-141-330-4771; ORCID number 0000-0003-1361-4645)

[7]These authors contributed equally to this work

[8]Co-senior authors

Running Head: CO_2-mediated control of stomata

ABSTRACT

Stomata of most plants close to preserve water when the demand for CO_2 by photosynthesis is reduced. Stomatal responses are slow compared to photosynthesis, and this kinetic difference erodes assimilation and water use efficiencies under fluctuating light. Despite a deep knowledge of guard cells that regulate the stoma, efforts to enhance stomatal kinetics are limited by our understanding of its control by foliar CO_2. Guided by mechanistic modelling that incorporates foliar CO_2 diffusion and mesophyll photosynthesis, here we uncover a central role for endomembrane Ca^{2+} stores in guard cell responsiveness to fluctuating light and CO_2. Modelling predicted and experiments demonstrated a delay in Ca^{2+} cycling that was enhanced by endomembrane Ca^{2+}-ATPase mutants, altering stomatal conductance and reducing assimilation and water use efficiency. Our findings illustrate the power of modelling to bridge the gap from the guard cell to whole-plant photosynthesis, and they demonstrate an unforeseen latency, or 'carbon memory', of guard cells that affects stomatal dynamics, photosynthesis and water use efficiency.

INTRODUCTION

The main pathway for CO_2 entry into the leaf for photosynthesis by the mesophyll cells is through the stomatal pore. Each stoma is surrounded by pairs of guard cells that regulate its aperture to balance the demand for CO_2 with the often opposing need to conserve water. The guard cells control the pore aperture by the uptake and loss of osmotic solutes, especially of K^+ and Cl^-, and by the synthesis and metabolism of small organics, notably malate (Mal), altering guard cell volume and turgor and thereby the size of the stomatal pore[1-4]. Environmental stimuli, especially light and the partial vapor pressure of water in the atmosphere, affect transport through a network of signalling pathways to regulate water and osmotic solute flux for stomatal aperture[2,5-8].

Much attention has been drawn to inputs closely tied to photosynthesis, the partial pressure of CO_2 in the atmosphere (pCO_2), and their impact on CO_2 within the air space of the leaf (pC_i). Stomata of most angiosperms close when pC_i rises, typically as photosynthetically-active light declines, to preserve water when the demand for CO_2 is reduced[2,4,7]. However, stomatal responses to light and CO_2 are slow by comparison with that of photosynthesis[2,9]. Variations in light during the day can degrade photosynthetic carbon assimilation and water use efficiencies (WUE, defined as the carbon gain per unit water loss), principally because stomatal responses generally lag behind changes in light[2]. Indeed, optogenetic manipulation of guard cell transport has shown that substantial gains in carbon assimilation and in WUE are possible by accelerating stomatal movements[9]. These studies underscore the need to understand how CO_2 affects guard cell mechanics and its integration with mesophyll-derived changes in pC_i in efforts to enhance stomatal kinetics.

Stomatal closing evoked by changes in pCO_2 and by the water-stress hormone abscisic acid (ABA) are associated with signalling via cytosolic pH[10,11], cytosolic-free Ca^{2+} concentration ($[Ca^{2+}]_i$)[12], protein kinases and phosphatases[1,13,14]. These signal cascades promote anion and K^+ efflux through concerted alterations in the activities of several ion transporters to reduce guard cell turgor, volume, and thereby stomatal aperture. Elevating pCO_2, like ABA, activates outward-rectifying K^+ channels such as GORK and Cl^- channels such as SLAC1, and it reduces the activity of the inward-rectifying K^+ channels in *Vicia* and the corresponding KAT1 and KAT2 channels in Arabidopsis guard cells[15-17]. Efforts to reconstruct putative CO_2 signal cascades of Arabidopsis[18-20] have highlighted a role for the SLAC1 anion channel, but these studies leave open questions about its mechanics and coordination with other transporters in the guard cell[1], and how these might be engineered to accelerate stomatal movements with photosynthetic demand for CO_2.

To address this challenge and gain further insights into stomatal control, we incorporated CO_2 within a mechanistic model of the guard cell coupled to mesophyll photosynthesis to explore stomatal integration with foliar carbon assimilation. The OnGuard

84 modelling platform encompasses guard cell transport, signalling, and essential metabolism,
85 accommodating foliar transpiration and successfully predicting emergent guard cell
86 behaviors across species, including Arabidopsis[16,21-24]. Using this platform to guide
87 experiments, here we uncover a critical role for endomembrane autoinhibited Ca^{2+}-ATPases
88 (ACAs) and Ca^{2+} cycling in short-term responsiveness under fluctuating light and pCO_2. The
89 findings demonstrate a latency, or 'carbon memory', in stomatal kinetics that erodes carbon
90 assimilation and water use efficiencies; they also illustrate the power of quantitative
91 mechanistic modelling to bridge the gap from guard cell transport to photosynthesis in the
92 whole plant.
93
94

RESULTS

Resolving a minimum set of regulatory targets for CO_2 in OnGuard3

Ultimately aperture, and hence the ensemble conductance, g_s, of stomata in the leaf to gaseous diffusion, is central to the feedback between photosynthetic CO_2 demand and its supply from outside. While the connection between photosynthesis and stomatal responses to pC_i within the leaf is not disputed, its mechanics are[1]. To examine potential mechanisms integrating pC_i with feedback to the guard cells, initially we incorporated CO_2 diffusion within the OnGuard platform[16,24] to generate OnGuard3.

Previously we identified a site, *p*, within the substomatal cavity behind the stomatal pore that describes the fractional resistance for water vapor diffusion from the mesophyll to the stomatal pore and from there to the atmosphere[25]. Hence, *p* defines the water vapor pressure within the substomatal cavity with which the guard cells equilibrate. To feed the demand of photosynthesis, CO_2 must diffuse along the same path but in the opposite direction, toward the mesophyll where it equilibrates with CO_2 in solution and diffuses across the cell membrane and into the chloroplast to be fixed into sugar[26-28]. We used this knowledge, incorporating the counterflux in CO_2 and the representation of *p* to define the fractional resistance to CO_2 diffusion from the atmosphere to the mesophyll and to calculate pC_i with which the guard cells equilibrate. pC_i was thus anchored by the CO_2 partial pressure outside and subject to the sink of the photosynthetic assimilation rate by the mesophyll inside the leaf (Figure 1 and Supplemental Appendix A1).

The OnGuard platform incorporates membrane ion transport, the metabolism of osmotically-active solutes, and their kinetic interactions with sufficient detail to describe and predict stomatal physiology[16,22-24]. Stomatal aperture and g_s are core outputs of the OnGuard platform and are determined by the combined operation of all of transport and metabolism within the model. For pC_i, which motivates changes in stomatal aperture via feedback not yet fully elucidated, this feedback must be represented by a mechanism engaging defined model components. Thus, each modelled mechanism represented a hypothesis under test, to be discarded, validated, or refined by comparisons between model predictions and experimental results.

A large body of evidence indicates that transmembrane solute transport in the guard cells normally drives stomatal movements[1,13]. We used the extant literature and global sensitivity analysis[29] to guide our initial construction of models incorporating pC_i as a modulator of guard cell membrane transport. These considerations highlighted contributions of endomembrane Ca^{2+}-ATPases (VCa-ATPase) and Ca^{2+} channel (VCa_{in}) activities, and to a lesser extent that of plasma membrane Ca^{2+}- and H^+-ATPases (Ca-ATPase, H-ATPase), the ALMT12 anion channel (ALMT) and TPK K^+ channel in stomatal closing (Supplemental Appendix A2). To these, we added the SLAC1, SLAH1 and SLAH3 (SLAC) anion channels,

the KAT1 and KAT2 (KAT) and GORK (GORK) K^+ channels at the plasma membrane, and the endomembrane malate and Cl^-/NO_3^- (VMAL, VCl) channels, and the FV K^+ (FV) channel, all of which are known either to be affected by CO_2 or associated with ABA-evoked stomatal closure[1,30,31] [a full list and parameter descriptions for each transporter in the OnGuard platform will be found in Hills et al[21] and Wang et al[16]].

We carried out systematic trials, simulating elevated pCO_2 steps from 400 to 1000 µbar and back again. These models retained the full complement of solute and transporter dependencies as well as the sensitivity to the partial water vapor pressure, described previously[16,22,23]. Dissolved CO_2 and the associated variable of cytosolic $[HCO_3^-]$ ($[HCO_3^-]_i$) were incorporated as ligands, assuming their equilibration with pC_i (Appendix A1). Similar results were obtained with dissolved CO_2 and with $[HCO_3^-]_i$, and we therefore focused on $[HCO_3^-]_i$ (hereafter implicit in reference to pC_i) which has been proposed as the effective species in SLAC channel regulation[32].

Dependencies on pC_i were introduced first to individual transporters and subsequently to transporters in combination, including the plasma membrane SLAC and ALMT anion channels, the KAT and GORK K^+ channels, the endomembrane VMAL, VCl, TPK and FV channels (see Supplemental Appendix A2 and Supplemental Table 2). These trials failed to show reductions in g_s and stomatal aperture, notably with any of the anion channels alone or in combination. Stomatal closure with elevated pCO_2 was recovered only if parameters defining VCa-ATPase or VCa_{in} activities were included as ligand targets. Suppressing VCa-ATPase or enhancing VCa_{in} activity with pC_i was sufficient to decrease g_s and stomatal aperture consistent with steady-state values reported previously[33,34]. However, we recovered rates of stomatal closure and g_s decline comparable with experimental data[32,35,36] (cf. Figure 2) only if pC_i additionally accelerated the kinetics defining VCa_{in} inactivation (Supplemental Figure S1 and Supplemental Appendices A2 and A3).

These findings identified both the endomembrane Ca^{2+}-ATPases and Ca^{2+} channels as important targets for stomatal response to pC_i. Adding pC_i dependencies to the SLAC, ALMT, and GORK channels to enhance these currents, additional to that promoted by $[Ca^{2+}]_i$ [37,38] - consistent with reports to date for GORK in vivo[15] and for SLAC1 on heterologous expression[14,20] - yielded small increases of less than 3% only in aperture and g_s kinetics. For consistency with these studies, we included the additional anion and K^+ channel targets with those of endomembrane Ca^{2+} transport in further simulations (see Supplemental Figure S2 and Supplemental Appendix A3).

OnGuard3 predicts a steep dependence of g_s and assimilation on pCO_2 and fluence rate and counterintuitive alterations in channel activities

Models constructed with OnGuard3, and incorporating pC_i sensitivity to endomembrane Ca^{2+} transport, faithfully reproduced experimental measurements of stomatal aperture, foliar stomatal conductance, g_s, and of pC_i dynamics, as well as photosynthetic carbon assimilation (Supplemental Figure S3), as functions of pCO_2 and fluence rate (Figure 2). Such behavior is consistent with the large body of evidence relating g_s to atmospheric pCO_2 and photosynthetic activity[1,2,5-8]. OnGuard3 replicated g_s kinetics and steady-state values to within 20% of the experimental means across a wide range of pCO_2 and fluence rates (see also below). Model outputs showed that stomatal closing with steps above 400 µbar CO_2 followed on a rise and partial recovery in pC_i (Figure 2a) and was accompanied by membrane depolarization (Figure 3a,b), elevated $[Ca^{2+}]_i$ (Figure 3c,d), parallel declines in the concentrations of the major osmotic solutes, K^+, Cl^- and Mal (Figure 3e-g), and a reduction in g_s (Figure 3h), guard cell turgor and stomatal aperture (Supplemental Figure S2d,e), as expected.

Increasing pCO_2 enhanced the activity of the GORK K^+ channels (Figure 4a,b) and reduced KAT channel activity in simulation and in vivo in Arabidopsis (Figure 4c,d), as observed in *Vicia*[16,22,39]. Suppression of the KAT channel activity arose from the elevated $[Ca^{2+}]_i$ (Figure 3c; see also Supplemental Figure S2) that is known to suppress the K^+ current[1,39]. In simulation, coordinate oscillations in $[Ca^{2+}]_i$ and membrane voltage were maintained until a new steady-state in aperture and g_s was approached (Figure 3a-d). Increasing pCO_2 is known to elevate $[Ca^{2+}]_i$ [12], with oscillations of 10-20 min duration in $[Ca^{2+}]_i$ facilitating solute efflux during the depolarised phase of each oscillatory cycle[22,39-41]. Model analysis (Supplemental Figure S2k-o) showed that the elevated $[Ca^{2+}]_i$ and its oscillation resulted from a cyclic influx of Ca^{2+} across the plasma membrane which promoted a much larger release of Ca^{2+} from endomembrane stores, so-called Ca^{2+}-induced Ca^{2+} release[1,42]. By contrast, increasing pCO_2 to 1000 µbar in simulation had only a marginal effect on pH_i (Supplemental Figure S2g) consistent with in vivo data showing that any effects are generally below the limit of resolution[15].

Counterintuitively, returning pCO_2 to its starting value in simulation resulted in an overshoot in KAT channel activity (Figure 4c, Supplemental Figure S2r) and could be ascribed to the relaxed $[Ca^{2+}]_i$ constraint on the K^+ current[1,22,39]. We carried out voltage clamp experiments to test this prediction, challenging guard cells of wild-type Arabidopsis during the experiments with buffer equilibrated to 1000 µbar CO_2. As predicted, elevating CO_2 in solution evoked reductions in KAT current and returning to 400 µbar CO_2 was followed by large overshoots in KAT activity (Figure 4d). Fitting the steady-state K^+ currents to a Boltzmann function (Figure 4d) showed that returning from 1000 to 400 µbar CO_2 enhanced KAT current with a maximum ensemble current conductance g_{max} rising from

0.38±0.02 to 0.76±0.04 mS cm^2 and evoked shifts in the voltage yielding half-maximal conductance, $V_{1/2}$, from -186±2 mV to -174±3 mV, respectively, relative to initial values (Figure 4c, *insets*). The response can be understood as a consequence of the $[Ca^{2+}]_i$ sensitivity of the K^+ current, but the overshoot in K^+ current and the enhanced channel activity evident in the shift of $V_{1/2}$ had not been identified before. The timescales of these experiments, typically 20-30 min for any one recording, precluded measurements to full recovery. However, the reversibility of the GORK current with pCO_2 steps validated OnGuard3 predictions (Figure 4a,b).

To assess $[Ca^{2+}]_i$ during pCO_2 elevation and recovery, we loaded Arabidopsis guard cells in epidermal peels with the dye Fura-Red and recorded dye fluorescence by confocal microscopy on excitation with 405 nm and 488 nm light. Measurements of $[Ca^{2+}]_i$ as the fluorescence ratio F_{405}/F_{488} were calibrated against similar recordings from guard cells permeabilized with the Ca^{2+} ionophore Ionomycin in the presence of defined and buffered Ca^{2+} concentrations. Measurements were carried out under continuous buffer flow before, during and after superfusion with buffer equilibrated with 1000 μbar CO_2. We found that elevating pCO_2 from 400 to 1000 μbar led to a substantial rise in $[Ca^{2+}]_i$ within the first 5 min and was followed by an undershoot in $[Ca^{2+}]_i$ on returning to 400 μbar CO_2 (Figure 4e-g), as predicted (Figure 3c). Dye bleaching over the time period of these recordings prevented measurements to full recovery and precluded resolution of the slower $[Ca^{2+}]_i$ oscillations evident in modelling[40] (Figure 3c). However, recordings from guard cells on the same epidermal peel 45 min later, and hence also exposed to the first pCO_2 step (Figure 4f,g), showed similar $[Ca^{2+}]_i$ responses to 1000 μbar CO_2, indicating that $[Ca^{2+}]_i$ recovered during this period.

Ca^{2+} stores determine a latency, or carbon 'memory', with light and pCO_2 steps

One major prediction of OnGuard3 models is that stomatal closure with elevated pC_i leads to a transient reduction in Ca^{2+} stores within the guard cell following Ca^{2+} release and the $[Ca^{2+}]_i$ oscillations that promote stomatal closure. The reduction in endomembrane Ca^{2+} stores (Figure 3d) and its recovery suggested a latency - in effect, a 'memory' - of previous closure events that could affect stomatal response when pC_i increased repeatedly. In simulation, repeated challenge with elevated pCO_2, when separated by intervals of 45 min and less, reduced endomembrane Ca^{2+} flux. The effect was store-mediated and displaced endomembrane Ca^{2+} channel gating from the free-running tonoplast voltage, thereby reducing subsequent Ca^{2+} release and $[Ca^{2+}]_i$ elevation (Supplemental Figure S4). As a consequence, stomatal closure in simulation was slowed when pCO_2 steps followed in close succession (Figure 5a,b).

We tested these predictions experimentally, initially with wild-type Arabidopsis, challenging plants with cycles of steps from 400 to 1000 μbar CO_2 separated by intervals at 400 μbar CO_2. As predicted, reducing the interval between steps to 30 min led to a significant reduction in $[Ca^{2+}]_i$ increases on the second and third challenges with 1000 μbar CO_2 (compare Figure 4g and Supplemental Figure S5). Furthermore, a slowing in stomatal closure to pCO_2 was evident (Figure 5a,b) when pCO_2 cycles to 1000 μbar were separated by intervals of 45 min or less, and matched closely the predicted latency halftimes for Ca^{2+} flux and g_s near 20 min (see also Supplemental Figure S4b).

Simulations also indicated that the effects on $[Ca^{2+}]_i$ elevations and stomatal kinetics might be greatly amplified if the population of endomembrane Ca^{2+}-ATPases was reduced to slow the recovery of Ca^{2+} stores (Supplemental Figure S4a,b). Assessing the consequences of short-term changes in stored Ca^{2+} is possible, even if their direct measurement is not. OnGuard3 does not distinguish among endomembrane Ca^{2+} stores and subsumes all endomembrane transport within the tonoplast[21,22]. Therefore we examined g_s in leaves of wild-type Arabidopsis and of the higher-order endomembrane Ca^{2+}-ATPase mutants, *aca4aca11* and *aca1aca2aca7*, that lack the predominant Ca^{2+}-ATPases at the tonoplast and at the endoplasmic reticulum, respectively. We also assessed g_s of the *aca4aca11* and *aca1aca2aca7* mutants complemented with *ACA11* and *ACA2*, respectively. The Ca^{2+}-ATPases at both membranes are functionally redundant and only the higher-order mutants display any phenotypes[43-46]. The *aca1aca2aca7* mutant has been reported to prolong evoked $[Ca^{2+}]_i$ elevations[46], although neither mutant has a significant effect on total foliar Ca^{2+} in the steady state[43-45], results that we confirmed (Supplemental Figure S6).

We used gas exchange measurements to assess the kinetics of stomatal closure while stepping between 400 and 1000 μbar CO_2 under continuous 200 μmol $m^{-2}s^{-1}$ PAR with periods of either 30 or 45 min between cycles of elevated pCO_2, following our prediction and findings in wild-type Arabidopsis (Figure 5a,b) of a cusp in slowed g_s kinetics with intervals near 45 min. In simulations, reducing endomembrane Ca^{2+}-ATPase activity to 40% or less of the wild-type greatly slowed g_s with cycles of elevated pCO_2 (Figure 5d and Supplemental Figure S4). In experiments, both *aca4aca11* and *aca1aca2aca7* mutants showed g_s kinetics that slowed significantly on repeated pCO_2 elevations, whereas the *ACA11* and *ACA2* complementations of *aca4aca11* and *aca1aca2aca7*, respectively, yielded g_s kinetics that were indistinguishable from wild-type plants (Figure 5c,d). Fitting these data to a first-order exponential function yielded more than a 2-fold decrease in the rate for g_s response on the second and third cycle of elevated pCO_2 compared to the first cycle for the *aca4aca11* and *aca1aca2aca7* mutants. When compared to the wild-type plants these rates of closure were reduced by a factor of 3, much as predicted in simulations. A comparison with repeated

cycles of steps between 200 and 0 μmol $m^{-2}s^{-1}$ light under constant 400 μbar CO_2 showed qualitatively similar reductions in g_s kinetics in the mutants (Supplemental Figure S7), consistent with a reduced demand on pC_i by carbon assimilation in the mesophyll.

In parallel experiments, we recorded $[Ca^{2+}]_i$ changes by confocal microscopy using Fura-Red, as before, while following treatments with repeated cycles of increased pCO_2. $[Ca^{2+}]_i$ elevations were largely indistinguishable between pCO_2 cycles in guard cells of wild-type plants (Figure 4e-g). However, increases in $[Ca^{2+}]_i$ in the *aca4aca11* and *aca1aca2aca7* mutants were slower initially to recover a resting $[Ca^{2+}]_i$ after steps to 1000 μbar CO_2 (Figure 5e,f and Supplemental Figure S8). More still, subsequent increases in $[Ca^{2+}]_i$ were significantly reduced on repeated cycles of increased pCO_2 in the mutants but not in their *ACA11* and *ACA2* complemented plants (Figure 5g and Supplemental Figure S8). These results lead us to conclude that recovery of the Ca^{2+} stores and its impact on endomembrane Ca^{2+} release introduces a latency in the response to repeated closing stimuli, in effect setting the timeframe for the latency and recovery in responsiveness of stomatal kinetics under fluctuating CO_2 and light.

Growth and water use efficiency are subject to the stomatal 'carbon memory'

Finally, we asked whether the latency in $[Ca^{2+}]_i$ elevations, their recovery, and the impact on stomatal kinetics might affect carbon assimilation and water use efficiency of the plant. As a measure of plant productivity, water use efficiency (WUE) is commonly defined as the amount of dry mass produced per unit water transpired and, thus, is strongly affected by light through its combined influence on carbon demand, pC_i, and on the associated rate of transpiration. Light commonly fluctuates in the natural environment, for example with changes in cloud cover during the day. Photosynthetic capacity tracks this light input. However, stomata generally respond over much longer timescales, leading to periods of suboptimal assimilation limited by stomatal conductance with a rise in fluence rate and to periods of high transpiration without corresponding assimilation when fluence rates decline. Because the *aca4aca11* and *aca1aca2aca7* mutants greatly reduced $[Ca^{2+}]_i$ elevations and slowed stomatal kinetics in response to repeated steps in pCO_2 and light, we predicted that growth and WUE of the mutants would be reduced under fluctuating light.

To test these predictions, we grew wild-type plants, the *aca4aca11* and *aca1aca2aca7* mutants, and their complementations under 50% relative humidity and two light regimes, each with cycles of 9 h:15 h L:D and the same total diel fluence. One set of plants (fixed) were given a constant daylight fluence rate of 140 μmol m^{-2} s^{-1}; a second set of plants (variable) were given daylight periods of fluctuating light, stepping at 1-h intervals between fluence rates from 20 to 200 μmol m^{-2} s^{-1} (see Methods). Both sets of plants were

subject to water limitation with the relative water content of the soil maintained at 15±5%. After 5 wk growth, the plants were harvested and WUE calculated using the accumulated dry aerial biomass divided by the total water applied over the growth period.

We found (Figure 6) that rosette area, WUE, and total dry biomass were only marginally reduced in the *aca4aca11* and *aca1aca2aca7* mutants compared to the wild-type plants when grown under the fixed light regime. Rosette area, WUE and dry biomass of wild-type plants and of the complemented lines were also slightly reduced under the variable light regime. However, all of the parameters were strongly reduced in the *aca4aca11* and *aca1aca2aca7* mutants when grown under the variable light regime. The decrease in WUE and biomass was not the consequence of alterations in photosynthetic capacity. Net CO_2 assimilation rates under saturating light (600 µmol m^{-2} s^{-1}) were unaffected in the *aca4aca11* and *aca1aca2aca7* mutant plants when compared to the wild type across the physiological range of pC_i (Supplemental Figure S9). These findings thus support a role for guard cell Ca^{2+} stores in maintaining carbon assimilation and the water use efficiency of the plant.

DISCUSSION

A substantial literature shows that stomatal conductance, g_s, in most plants alters in inverse relation with the partial pressure of CO_2 within the leaf, pC_i, and its reduction by mesophyll photosynthesis in the light. These observations make intuitive sense in balancing the demand for CO_2 by photosynthesis against the need to prevent leaf drying, but they leave open the mechanism by which stomata achieve this balance in opening and closing. Like the response to ABA, CO_2 has a broad impact on guard cell transport[1], much with plausible connections to CO_2-evoked $[Ca^{2+}]_i$ increases[12]. Elevated CO_2 has been associated with altered activities of plasma membrane K^+ and Cl^- channels, H^+-ATPases, and the tonoplast TPK1 K^+ channel, although each arises through secondary regulation[15,47-49]. Studies of SLAC1 in Arabidopsis have highlighted the anion channels as a potential target for the direct action of pC_i (and HCO_3^-) in stomatal closure[13,14,20]. However, the HCO_3^- concentrations needed to enhance the SLAC1 activity in isolation[20,32] - in excess of 10 mM - bear no relation to the HCO_3^- concentrations at physiological pC_i that regulate stomatal conductance, typically between 50-200 μM[2,7,8,33,34,50], and bring into question the physiological relevance notably of the SLAC1 responses reported on heterologous expression to date[14]. Thus, the challenge has remained to identify a core and unifying mechanism that can account for the regulation of stomatal aperture and conductance associated with pC_i and carbon assimilation by the mesophyll.

We combined predictive systems modelling with experimental analysis to address this challenge and, in doing so, have uncovered an unexpected mechanism conferring a latency - what we describe as a 'carbon memory' - on stomatal kinetics with fluctuations in light and CO_2. We incorporated within the OnGuard platform[16,21,22,24] the diffusion of CO_2 in the leaf coherent with that of water vapor with which the guard cells equilibrate to sense changes in the water vapor pressure difference between the leaf and atmosphere[16,25]. The strength of this approach is that it unifies the mechanics of stomatal response to CO_2 along with photosynthetic carbon assimilation and transpiration within a single, computational framework that scales naturally from the microscopic processes of solute and water transport in the guard cell to the macroscopic relations of gas exchange and carbon assimilation in the leaf and whole plant. OnGuard3 encapsulates all of the guard cell membrane transport and metabolism pertinent to stomatal movements with quantitative kinetic detail[16,21,22]. Thus, the potential mechanics for CO_2 to regulate guard cell ion transport, metabolism, and g_s, are available to test by assigning pC_i dependencies to one or more of these processes. In short, each modelled mechanism becomes a hypothesis under test, to be discarded, validated, or refined by comparisons between model predictions and experimental results[51].

OnGuard3 accurately described the experimentally-determined dependence of stomatal aperture and g_s on pCO_2 and carbon assimilation, and it produced sensible rates of photosynthetic fixation with g_s, provided only that pC_i was assigned to the activities of two transporters affecting endomembrane Ca^{2+} sequestration. Required was that pC_i suppress the VCa^{2+}-ATPase and, equally that it accelerate the cyclic inactivation of the VCa_{in} Ca^{2+} channels for endomembrane Ca^{2+} release (Supplemental Appendix A2 and A3). Incorporating the dependencies of VCa_{in} and VCa^{2+}-ATPase on pC_i in OnGuard3 accurately predicted, among others, the counterintuitive responses of guard cell K^+ channels to steps in pCO_2 to 1000 μbar and its recovery as well as undershoots in $[Ca^{2+}]_i$ (Figure 4). These are characteristics expected of a unified framework connecting guard cell transport to CO_2 within the leaf: each response arises directly from corresponding alterations in pC_i as it is affected by gaseous flux through the stomatal pore and by the photosynthetic sink of carbon assimilation.

We stress that the central role for endomembrane Ca^{2+} transport uncovered by OnGuard3 does not discount additional effects on the plasma membrane Ca^{2+} channels, AHA1 H^+-ATPase, SLAC1, GORK or tonoplast TPK1 channels[1,15,18-20,47-49]. It suggests, however, that such actions are secondary to the impact of pC_i on Ca^{2+} homeostasis within the guard cell and the effects of elevating $[Ca^{2+}]_i$ on the subset of $[Ca^{2+}]_i$-sensitive transporters[1]. Indeed, elevating $[Ca^{2+}]_i$ is essential for CO_2 (and HCO_3^-) to enhance the SLAC1 current in vivo; by comparison with $[Ca^{2+}]_i$, the effects reported to date on the heterologously-expressed SLAC1 channel of varying HCO_3^- are modest[15,20,52]. The OnGuard3 analysis also clearly indicates that pC_i regulation of SLAC1, alone and together with ALMT12, is not sufficient to drive stomatal closure. This prediction accords with past experimental evidence showing that coordinate regulation of several transporters, including the H^+-ATPases, is important for stomata to closure[1,53]. In short, SLAC1 is not a 'master switch' but is one of several ion transporters that must be regulated coordinately to facilitate stomata closure.

Ca^{2+} stores delineate a stomatal 'carbon memory' linked to photosynthesis

Most remarkable was the unexpected prediction of a decay in kinetics as stomata cycled between closing and opening with repeated steps in light and pCO_2 and its connection to Ca^{2+} stores in the guard cell. Behind this prediction, simulations showed transient declines in endomembrane Ca^{2+} stores and the capacity for Ca^{2+} release that introduced a latency - in effect, a 'carbon memory' - in the recovery of stomatal responsiveness. OnGuard3 predicted that this 'carbon memory' should be enhanced by reducing the population of endomembrane Ca^{2+}-ATPases, thereby prolonging the delay in recovering stomatal responsiveness (Figure 7). Comparing g_s and guard cell $[Ca^{2+}]_i$

dynamics confirmed these predictions when comparing the *aca4aca11* and *aca1aca2aca7* Ca^{2+}-ATPase mutants impaired in Ca^{2+} sequestration with their *ACA11* and *ACA2* complementations and wild-type plants.

Our predictions and experimental validations accord with the primary importance to cellular $[Ca^{2+}]_i$ balance of endomembrane Ca^{2+} transport and the comparatively minor role of Ca^{2+} entry through plasma membrane Ca^{2+} channels[29,39,54-56]. Best estimates[22,40] indicate that more than 95% of the Ca^{2+} entering the cytosol during $[Ca^{2+}]_i$ elevations comes from endomembrane stores. By contrast with the common focus to date on pathways for Ca^{2+} influx to the cytosol[57], our findings emphasize also the importance of Ca^{2+} sequestration and its kinetics to the temporal characteristics of $[Ca^{2+}]_i$ increases.

The discovery of a latency and its dependence on Ca^{2+} sequestration are all the more remarkable, because previous studies had indicated that the *aca* mutants have no significant effect on total foliar Ca^{2+} in the steady state[43,44] (Supplemental Figure S6). Yet, as predicted, repeated steps to 1000 μbar CO_2 showed very significant decays in $[Ca^{2+}]_i$ elevations and g_s kinetics of the *aca4aca11* and *aca1aca2aca7* mutants. Similar results in g_s kinetics were obtained on repeated steps in light intensity, as expected for a behaviour mediated through pC_i. Furthermore, this decay in stomatal kinetics translated to a reduction in carbon assimilation and water use efficiency under fluctuating light conditions mimicking those frequently observed in the field (Figure 6).

These actions clearly arise as emergent properties of transport in the guard cell and become evident only through a mechanistic model spanning scales from the guard cell membrane to gas exchange of the whole plant. Our results not only illustrate the mechanistic connection of guard cell transport to carbon assimilation through $[Ca^{2+}]_i$, but they point to a role for guard cell Ca^{2+} stores in adjusting stomatal response to the recent history of pC_i. Like an 'after image' that impairs our vision on looking into a bright light, we can think of the stomatal 'carbon memory' as temporarily desensitizing guard cells to environmental fluctuations that repeatedly elevate pC_i. The findings thus place the Ca^{2+}-sequestering ATPases and the, as yet unidentified, endomembrane Ca^{2+} channels at the heart of an adaptive signalling network regulating CO_2 flux for photosynthesis (Figure 7). They demonstrate this 'carbon memory' as an important factor that tempers stomatal responses to fluctuating photosynthetic rates, such as may occur as clouds pass overhead, dampening the subsequent kinetics of closure. It is salutory that damped oscillations in stomatal aperture are widely documented across a number of species including Arabidopsis; the phenomenon has been associated primarily with water relations and the vapor pressure difference between the leaf and atmosphere, but it depends also on the background of photosynthetic activity and, hence, on light and pC_i [58-62].

Our findings also highlight guard cell Ca^{2+} sequestration and the endomembrane Ca^{2+}-ATPases as potential targets for bioengineering to enhance carbon assimilation along with water use efficiency through Ca^{2+} cycling kinetics. Much interest has centered ways of improving the water use efficiency of crops without a cost in photosynthetic carbon assimilation[63,64]. In principle, one approach relies on accelerating stomatal kinetics with light, and hence with pC_i, in order to better match stomatal responses with that of photosynthesis in a fluctuating environment. Manipulating guard cell K^+ transport by expressing a synthetic, light-gated K^+ channel has been shown successful as a route to this objective[9]. Manipulating the 'carbon memory' through the expression and characteristics of endomembrane Ca^{2+}-ATPases may prove still more effective.

Equally, OnGuard3 presents an opportunity to revisit the mathematical frameworks of canopy and global ecosystem analysis[26,65-70]. In the modelling context, these frameworks encapsulate the activities of plants centered on the single parameter of the stomatal conductance. As stomata mark the interface between the plant and atmosphere for both carbon and water exchange, such descriptions make intuitive sense, but they generally omit stomatal physiology. Stomatal responsiveness instead is subsumed within a phenomenology of empirical constraints, including theoretical maxima for stomatal aperture, g_s, photosynthesis, and the availability of water[26,71,72]. As Berry et al[26] noted a decade ago, "the decisions 'made by' stomata emerge as an important and inadequately understood component of these models." Connecting these higher-order frameworks with the biology of guard cells and the great depth of knowledge about how they work, as encapsulated within OnGuard3, is sure to yield new insights into the patterns of carbon and water circulation in the face of global changes in atmospheric CO_2 and temperature[73,74].

Finally, we stress that our discoveries are only a small sample of the predictions that arise from OnGuard3. Our results address a regulatory network that clearly is sufficient to explain the primary kinetic responses of stomata to pC_i in Arabidopsis. Their experimental validations underscore a tight interweaving of guard cell physiology and photosynthetic carbon flux with endomembrane Ca^{2+} transport in vivo. The OnGuard platform has proven equally successful in predicting the behaviors of guard cells and stomata in other species[21,22,40]. The capacity of OnGuard3 to connect the microscopic processes of the guard cell with carbon and water use by the whole plant opens new ways to addressing many other aspects of stomatal physiology, and is certain to yield greater understanding of the complex processes controlling foliar gas exchange.

MATERIAL AND METHODS

Growth and whole-plant physiology

Arabidopsis thaliana Col-0 wild-type, the *aca4aca11* and *aca1aca2aca7* mutants[43,44], *ACA11*-complemented *aca4aca11*, and *ACA2*-complemented *aca1aca2aca7* mutant plants were grown on 18:22 °C with light:dark cycles as indicated and gas exchange measurements were carried out using LICOR 6800 gas exchange systems (Lincoln, USA) as described previously[9,16,53]. All plants were analysed on at least three separate days at the same time of the relative diurnal cycle and were corrected for leaf area using ImageJ v.1.51h[75].

For analysis of rosette area, biomass, WUE and total Ca^{2+}, seedlings were transferred to 5-cm pots 2 wk post-germination and grown for a further 5 wk under watering regimes as indicated and 9 h:15 h L:D with a total daily fluence of 4.54 mol m^{-2}. For comparisons between constant and fluctuating light regimes, plants were grown either under constant light of 140 µmol m^{-2} s^{-1} or under light that fluctuated at 1-h intervals between fluence rates from 20 to 200 µmol m^{-2} s^{-1} (hourly sequence in µmol m^{-2} s^{-1}: 200, 20, 200, 80, 180, 200, 20, 200, 160). Rosette areas were analyzed from calibrated images and were harvested and fresh and dry weights determined using protocols described previously[9]. Dried samples were analyzed for total Ca^{2+} after extracting in 2M HCl for 7 d and centrifugation to remove particulates. Ca^{2+} in the supernatant was determined by flame photometry, calibrated against known standards, and related to tissue volume assuming 1:1 (ml:gm) relation. Soil water content was monitored using a ML3 moisture sensor (DeltaT Devices, Cambridge UK) and plants watered at 2-d intervals to maintain 10±5% soil water content.

Ca^{2+}-ATPase complementation

The higher order knockout *aca1aca2aca7(aca1-7/2-3/7-5*) *and aca4aca11 (aca4-3/11-5)* were generated in the Col-0 background by combining T-DNA insertions from public collections[76-78]: *ACA1* (At1g27770), *aca1-7* (GABI_095C01); *ACA2* (At4g37640), *aca2-3* (SALK_082624); *ACA7* (At2g22950), *aca7-5* (SALK_132552); *ACA4* (At2g41560), *aca4-3* (SALK_029620); and *ACA11* (At3g57330), *aca11-5* (Sail_269_C07) to establish the loss-of-function mutations. The single and higher-order *aca1aca2aca7 and aca4aca11* mutants, their stable complementations with *ACA2* and *ACA11* transgenes, and their phenotypes are described elsewhere[43,46].

Guard cell electrophysiology and Ca^{2+} recording

Currents from intact guard cells in epidermal peels were recorded by voltage clamp using double-barrelled microelectrodes and Henry's EP suite (Y-Science, Glasgow, UK). All

recordings were carried out under continuous superfusion with 1, 10, and 30 mM KCl in 5 mM Ca^{2+}-MES, pH 6.1 ($[Ca^{2+}]$ = 1 mM)[16,23] equilibrated to 400 and 1000 μbar CO_2 [15]. Voltage was clamped in cycles with a holding voltage of -100 mV and steps either to voltages from -100 to -240 mV (KAT) or to voltages from -100 to +50 mV (GORK). Currents were analyzed using Henry's EP suite (Y-Science, Glasgow) and SigmaPlot 11 (Systat Software, Inc., USA) as described previously[15,79,80], and steady-state currents were fitted by joint, non-linear least-squares using the Boltzmann function (see Figure 4 legend).

Cytosolic-free Ca^{2+} concentration ($[Ca^{2+}]_i$) was recorded by confocal fluorescence microscopy from guard cells in epidermal peels under continuous superfusion with the same buffers equilibrated to 400 and 1000 μbar CO_2. Guard cells were preloaded with the Ca^{2+}-sensitive dye Fura Red by incubation in 50 μM Fura Red as the free acid dissolved in 40 mM glycine buffer, pH 3.6, with 10 mM KCl. Low pH treatment destroyed the epidermal cells that survived peeling, leaving the guard cells intact[81,82] as judged visually and by stabilization of resting $[Ca^{2+}]_i$. Images were collected using standardized settings with a Leica SP8-SMD confocal microscope equipped with 20x/0.85NA and 40x/1.3 NA objectives. Fluorescence was collected over 570-650 nm after excitation with 405 nm and with 488 nm laser light at 30-s intervals. $[Ca^{2+}]_i$ was determined from the fluorescence ratio F_{405}/F_{488} using ImageJ v.1.51h[75] after correcting for background fluorescence from epidermal peels prior to Fura-Red loading. The F_{405}/F_{488} ratio was calibrated against guard cells loaded with Fura Red, permeabilized with 10 μM Ionomycin[83], and superfused with defined Ca^{2+} concentrations between 0.01 and 100 μM.

OnGuard3 modelling

OnGuard3 was built on the HoTSig platform[21,22], including the extension for stomatal transpiration of OnGuard2[16], separate assignments of blue and red light[29], and the constraint imposed by cells surrounding the guard cells[24]. OnGuard3 incorporates CO_2 diffusion between the atmosphere and interior of the leaf to determine the partial pressure of CO_2 at site *p*, defining pC_i, within the substomatal cavity with which CO_2 in guard cells equilibrate (see Appendix A1). OnGuard3 models were driven through a diurnal light:dark cycle as before[16,22,23] with steps in pCO_2 and light imposed on this cycle as indicated, and all model outputs were derived from this cycle. Constant apoplastic solute contents were defined, and primary, energy-dependent transport, sucrose and malic acid synthesis within the guard cell were coupled to light as before[16,21,23]. Light input also contributed to the rate of carbon fixation by the leaf mesophyll and, hence, to the sink for CO_2 within the leaf according to established relationships between light, CO_2 and carbon assimilation[84,85] (see Supplemental Appendix A1). All other model parameters were fixed. The properties of the individual

transporters, metabolism and buffering reactions thus responded only to changes in model variables arising from the parameters encoded in the model (Supplemental Appendix A3). OnGuard3 and the models for wild-type and *aca* mutant Arabidopsis are freely available for academic users for download from www.psrg.org.uk.

Statistics

Results are reported as means ±SE of *n* observations. Significance was determined by Analysis of Variance (ANOVA), as appropriate, with post-hoc analysis (Student-Neumann-Keuls, Holm-Sidek and Tukey), and is indicated at $P<0.05$ unless otherwise stated. Note that models built on ordinary differential equations, such as those of OnGuard3, will faithfully reproduce a given set of outputs time and again for any one set of parameters. Statistical analysis of these outputs is therefore meaningless.

Acknowledgements: This work was supported by BBSRC grants BB/L001276/1, BB/L019205/1, BB/M001601/1, and BB/N01832X/1 to MRB and by National Science Foundation grant IOS 1656774 to JFH. YW was supported by the National Science Foundation of China grant 31871537 and the Central Universities Fundamental Research Fund 2020XZZX002-21. FS-A was supported by a Lord Kelvin and Adam Smith PhD studentship. We thank Amparo Ruiz-Pardo for help in plant maintenance.

Author contributions: MRB, AH, and VLL conceived the work and developed the model platform; AH encoded the platform; MRB, MJ, BH and YH resolved the models; MJ, JS, and YH carried out gas exchange and aperture measurements; FS-A, ND, and MRB carried out growth studies, biochemical and Ca^{2+} analyses; YW and FS-A carried out voltage clamp experiments, and MJ, YH and FS-A analyzed the results with MRB; MRB wrote the manuscript with MJ, AH, FS-A and VLL; all authors edited and approved the manuscript.

Competing interests: The authors declare no competing interests.

Data and code availability: Data generated and analysed during this study are included in this published article, its supplementary information files, and are also available on reasonable request to the corresponding author. The OnGuard3 platform and the model parameter sets as binary code described herein are freely available to academic users and may be downloaded from www.psrg.org.uk

581

582 Appendix A1. **Incorporating CO_2 diffusion and assimilation in OnGuard3**

583 Appendix A2. **Analysis of pC_i dependencies in OnGuard3**

584 Appendix A3. **OnGuard3 model parameters for wild-type and *aca* mutant Arabidopsis**

585

586 Supplemental Fig. S1. **OnGuard3 reveals a critical dependence on endomembrane Ca^{2+}**
587 **release and resequestration to drive stomatal closure with the partial pressure of CO_2**
588 **(pCO_2).**

589 Supplemental Fig. S2. **OnGuard3 outputs for guard cell pH, Ca^{2+}, osmotic solute**
590 **transport and Mal synthesis of the wild type.**

591 Supplemental Fig. S3. **Steady-state of carbon assimilation rate (*A*) and its dependence**
592 **on pCO_2 and PAR fluence rate.**

593 Supplemental Fig. S4. **Reducing endomembrane Ca^{2+}-ATPase activity in OnGuard3**
594 **suppresses cytosolic-free $[Ca^{2+}]$ ($[Ca^{2+}]_i$) oscillations and mean $[Ca^{2+}]_i$, and enhances**
595 **the latency in net endomembrane Ca^{2+} release.**

596 Supplemental Fig. S5. **Reducing the interval between 100 μbar pCO_2 steps suppresses**
597 **cytosolic-free $[Ca^{2+}]$ elevations.**

598 Supplemental Fig. S6. **Total foliar Ca^{2+} content is unaffected by mutation of**
599 **endomembrane *ACA* Ca^{2+}-ATPases.**

600 Supplemental Fig. S7. **Latency in g_s relaxation with light is strongly affected in mutants**
601 **lacking endomembrane Ca^{2+}-ATPases.**

602 Supplemental Fig. S8. **Repeated challenges with high partial pressure of CO_2**
603 **(pCO_2) transitions uncover a latency in the recovery of $[Ca^{2+}]_i$ elevations.**

604 Supplemental Fig. S9. **Erosion in the biomass of Ca^{2+}-ATPase mutant Arabidopsis is**
605 **not related to a reduction in photosynthetic capacity.**

606

607

608

609

610 Figure Legends

611

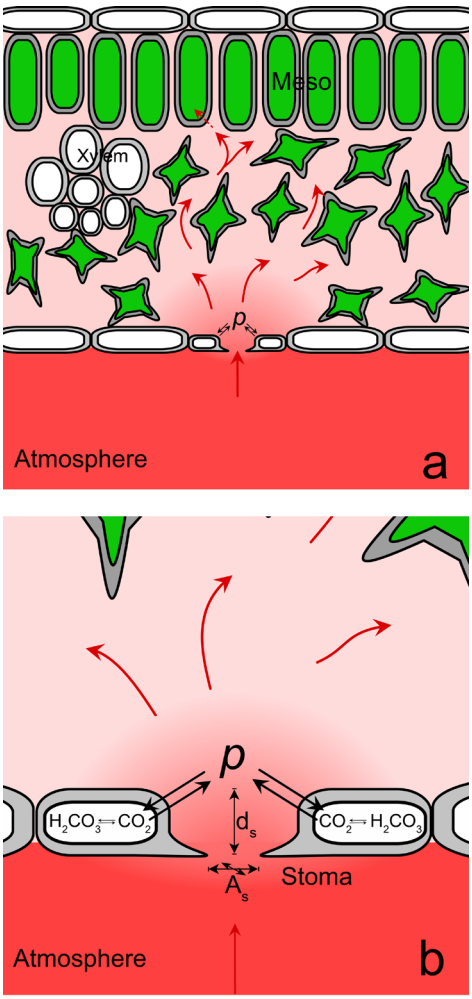

Figure 1. **Schematic of CO_2 diffusion from the atmosphere, through the stomatal pore (stoma) and point *p* near the inner mouth of the pore, to the CO_2 sink of photosynthesis in the mesophyll (meso) of the leaf**.

Shown are a transection of the leaf (a) and expanded schematic of the pore (b). Diffusion within the leaf and the stomatal frequency over the epidermal surface ensures the major drop in partial pressure of CO_2 between the atmosphere and mesophyll occurs across the stomatal pore[86,87]. In the light, gaseous CO_2 enters through the stomatal pore (A_S indicated, defined by the width and breadth of the pore; d_s defined by the depth of the pore), driven by diffusion towards a lower pCO_2, to establish a steady-state gradient (indicated by the red background shading; red arrows indicate direction of flow) with a reduced pCO_2 at *p*, defining pC_i within the leaf. Mathematically, *p* represents all points midway along the resistance pathway for diffusion between the atmosphere and the mesophyll and can be thought of as the average of the pCO_2 gradient centered over the guard cell which exchanges with CO_2 in solution and equilibrates with aqueous H_2CO_3 in the guard cell.

634

635

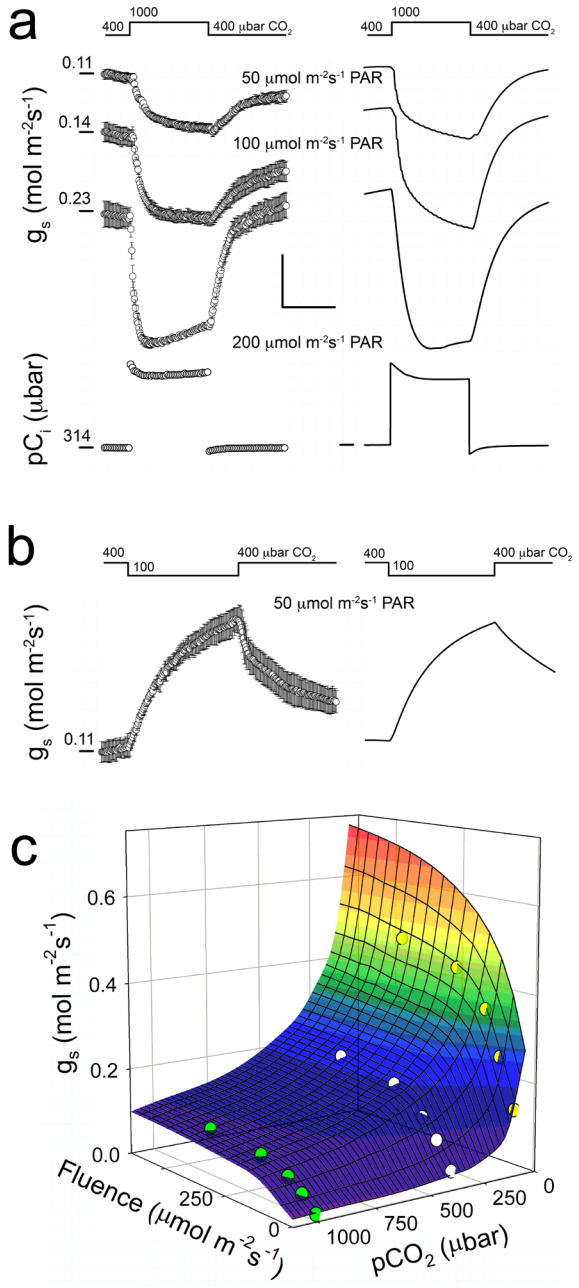

Figure 2. **OnGuard3 reproduces stomatal conductance (g_s) and its dependence on the partial pressure of CO_2 in the air (pCO_2) and light for photosynthesis in Arabidopsis.** (a) g_s behavior with pCO_2 steps between 400 and 1000 µbar CO_2 and with 50, 100 and 200 µmol $m^{-2}s^{-1}$ photosythetically-active radiation (PAR), as indicated. Experimental data (*left*) and model outputs (*right*) determined under well-watered conditions and 70 %RH[16]. Experimental data and model outputs are scaled to common axes and pairs offset vertically with values indicated (*left*). Scale bar: vertical, (g_s) 0.05 mol $m^{-2}s^{-1}$ or (pC_i) 350 µbar; horizontal, 1 h. Experimental data are means±SE of n≥3 independent experiments. Experimental and model calculations for internal CO_2 (pC_i) are included below for 200 µmol $m^{-2}s^{-1}$ PAR. (b) Experimental data (*left*) and model outputs (*right*) for g_s with pCO_2 steps between 400 and 100 µbar CO_2 and with 50 µmol $m^{-2}s^{-1}$ PAR. Experimental data and model outputs are scaled to common axes with the same scaling as in (A). (c) Steady-state of g_s and its dependence on pCO_2 and PAR determined from the OnGuard3 model (surface plot) and overlaid with experimental measurements (open symbols: green, white, yellow for 1000, 400 and 100 µbar CO_2, respectively) from Arabidopsis, including the data in (a) and (b). The corresponding experimental and modelled rates of photosynthetic carbon assimilation are shown in Supplemental Figure S3. Model parameters are summarised in Supplemental Appendix 3.

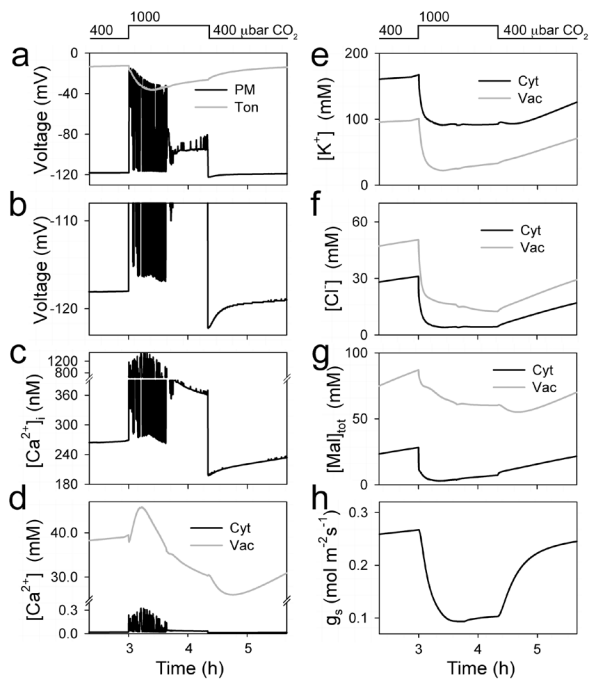

Figure 3. **OnGuard3 predicts an elevation in cytosolic free $[Ca^{2+}]$ ($[Ca^{2+}]_i$) on steps to 1000 μbar CO_2 and an undershoot in $[Ca^{2+}]_i$ on its return.**

Model parameters as in Figure 2 and summarised in Supplemental Appendix 3, with 200 μmol $m^{-2}s^{-1}$ photosythetically-active radiation (PAR). Plotted are (a, expanded scale in b) the plasma membrane and tonoplast voltages, (c) $[Ca^{2+}]_i$, (d) total cytosolic and vacuolar (endomembrane) Ca^{2+} concentrations, (e) $[K^+]$, (f) $[Cl^-]$, and (g) total malate [Mal] concentrations in the cytosol and vacuole, with (h) stomatal conductance (g_s) replotted from Figure 2 for reference (see also Supplemental Figure S2). Oscillations in $[Ca^{2+}]_i$ and plasma membrane voltage, and associated oscillations in other flux outputs, accelerate stomatal closing[40] by facilitating net efflux of solute. Note the decline in vacuolar (endomembrane) $[Ca^{2+}]$ (d) with pCO_2 elevation.

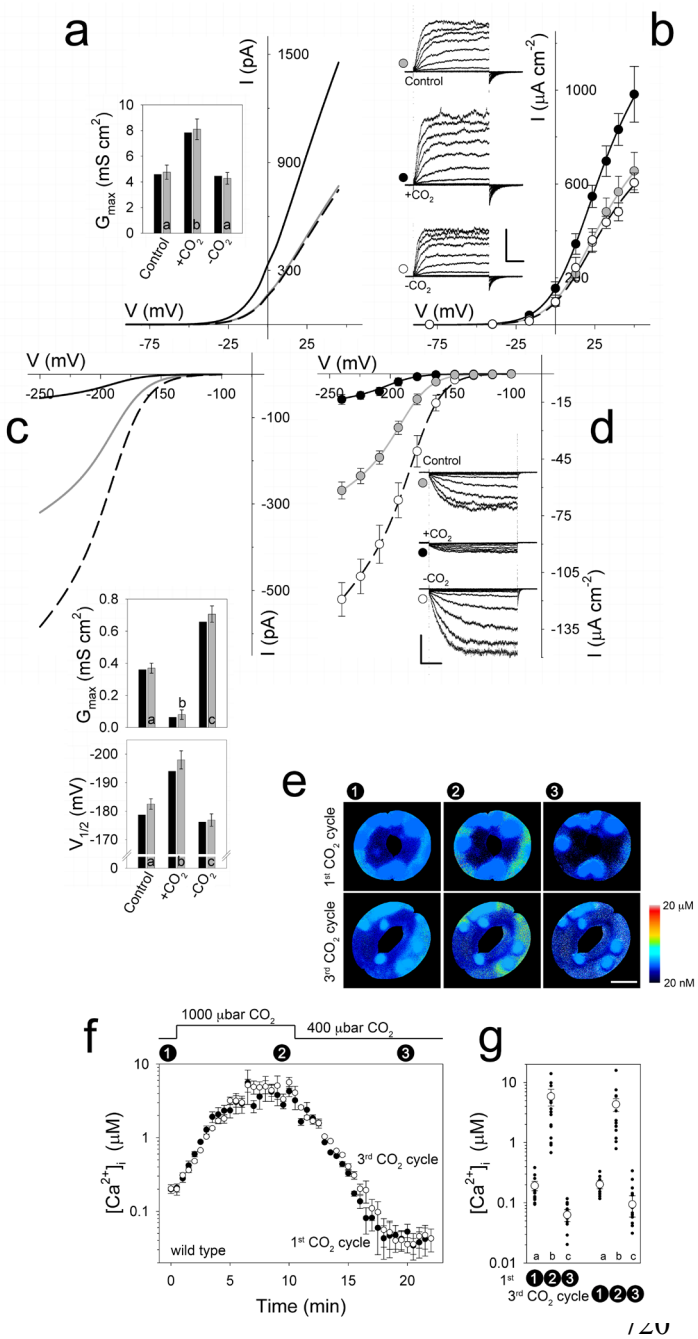

Figure 4. **pCO_2 elevation and its recovery identify a hysteresis in cytosolic-free $[Ca^{2+}]$ ($[Ca^{2+}]_i$) and K^+ channel activities predicted with OnGuard3.**

(a-d) OnGuard3 outputs (a,c) and experimental recordings (b,d) for the outward-rectifying (GORK, a,b) and inward-rectifying K^+ currents (KAT, c,d) before (Control, grey lines and symbols), 3 min into a step to 1000 µbar CO_2 (+CO_2, solid black lines and symbols), and 5 min after returning to 400 µbar CO_2 (-CO_2, dashed black lines and open symbols). Steady-state currents (b,d) from wild-type Arabidopsis guard cells recorded under voltage clamp in 5 mM Ca^{2+}-MES, pH 6.1, with 30 mM KCl and clamped from a holding voltage in steps from -100 mV to +50 mV (b) for GORK and from -100 to -240 mV (d) for KAT. Note the overshoot on recovery for KAT that are predicted outcomes of its dependence on $[Ca^{2+}]_i$ [16,23,39]. Data are means ±SE of n≥6 independent experiments. Curves are non-linear least-squares fittings carried out jointly for each current to the Boltzmann function

$$I = G_{max} \cdot (V-E_K)/(1+e^{\delta F(V-V_{1/2})/RT}) \quad [1]$$

where G_{max} is the maximum ensemble conductance, V is the voltage, $V_{1/2}$ is the voltage at which the ensemble conductance $G=0.5 \cdot G_{max}$, δ is the voltage sensitivity coefficient of the channel, E_K is the equilibrium voltage for K^+, and F is the Faraday constant. Fittings yielding

common voltage-sensitivity coefficients (δ) of 1.98±0.04 and 1.85±0.06 for KAT and GORK, respectively, and a common mid-point voltage ($V_{1/2}$) for GORK of +13±2 mV.
Insets: (a,c) Fittings to Eqn [1] of model (black bars) and experimental (grey bars) data for GORK (a) and KAT (c) indicating the varying parameters of G_{max} and conductance midpoint voltage $V_{1/2}$. Model data scaled for a surface area of 300 μm^2. Letters indicate significant differences (P<0.02). (b,d) Representative clamp current traces from one guard cell cross-referenced by symbol. Scales, 400 $\mu A\ cm^{-2}$ (GORK) and 50 $\mu A\ cm^{-2}$ (KAT) vertical, 1 s horizontal.
(e-g) Cytosolic-free $[Ca^{2+}]$ ($[Ca^{2+}]_i$) recorded from Arabidopsis guard cells pre-loaded with the Ca^{2+}-sensitive fluorescent dye Fura-Red and challenged with 1000 μbar CO_2. Images (e) and timecourse of measurements (f) for the guard cells of two stomata from the same epidermal peel challenged with pCO_2 steps separated by 45-min intervals. Images corresponding to the first and third steps pCO_2 steps are pseudo-color coded for $[Ca^{2+}]_i$ (scale, *right*). The light-shaded structures correspond to chloroplasts and were omitted from analysis. Image scale bar, 5 μm. Timecourse data (f) are means ±SE of measurements from n≥6 points around the periphery of each guard cell pair. Analysis of the timecourses (f) and endpoints (g) for $[Ca^{2+}]_i$ recorded from n≥11 independent experiments show a highly significant rise in $[Ca^{2+}]_i$ with pCO_2 elevation and undershoot on its recovery in each case. Time points are cross-referenced to the experimental protocol (g, *above*) by the circled numbers. Filled symbols in (g) are individual experimental data with means ±SE indicated by the open symbols and error bars. Letters indicate significant differences (P<0.02).

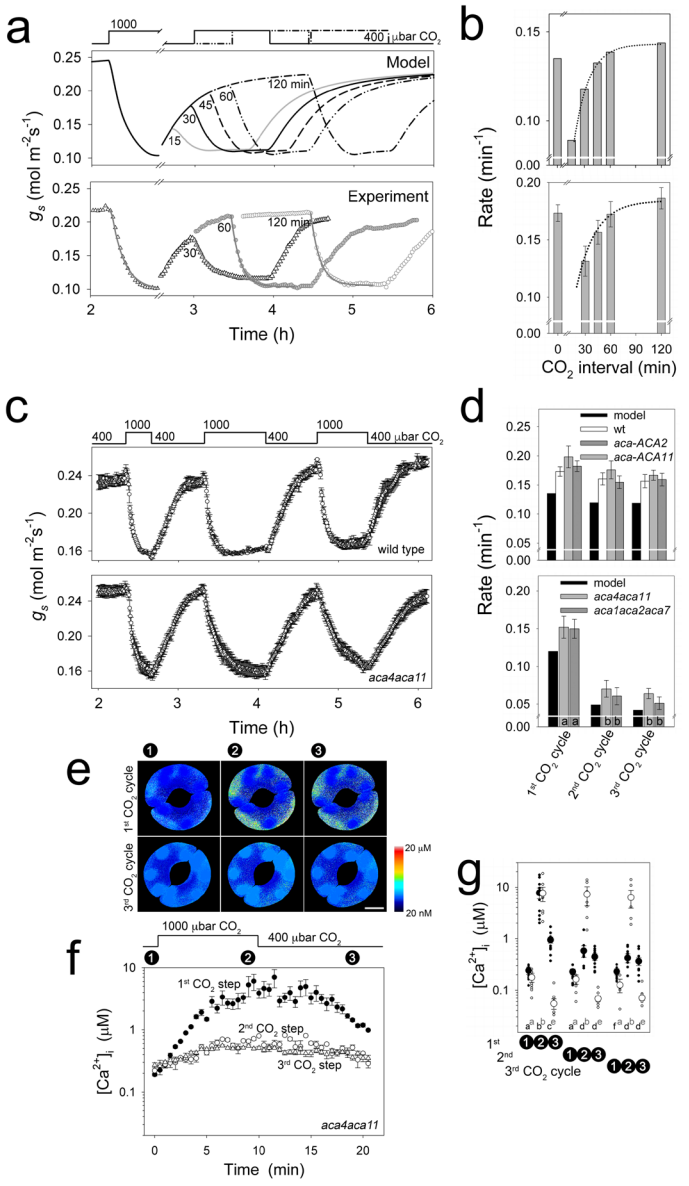

Figure 5. **Repeated pCO_2 challenge uncovers a latency in stomatal kinetics that depends on guard cell endomembrane Ca^{2+} stores.**

(a,b) OnGuard3 modelling (*above*) and experimental data from wild-type Arabidopsis (*below*) show a latency in responsiveness that slows stomatal closing and g_s kinetics on second exposure to elevated pCO_2. Initial 30-min steps from 400 to 1000 µbar CO_2 was followed by recovery intervals of 15-120 min at 400 µbar CO_2, as indicated, before a second 60-min step to 1000 µbar CO_2. Experimental data are of three plants with g_s kinetics fitted to a single exponential function (grey lines)[88]. Analysis of g_s relaxations with 1000 µbar CO_2 steps (b) are from n≥6 independent experiments including the data of (a). Model values were taken directly from simulation. Fittings of g_s rates with recovery period (b, dotted lines) yielded halftimes of 12±1 and 15±3 min for model (*above*) and experimental (*below*) latencies, respectively.

(c,d) Latency in g_s relaxations with pCO_2 is strongly affected in mutants lacking endomembrane Ca^{2+}-ATPases. Wild-type (*above*) and *aca4aca11* mutant (*below*) Arabidopsis plants were challenged with steps from 400 to 1000 µbar CO_2 separated by 45-min intervals at 400 µbar CO_2, as indicated. Data in each case are from n≥5 independent experiments (c) with rates determined as in (a). A summary of g_s kinetics (d) is shown for three successive pCO_2 steps (grey bars) for the wild-type and *ACA11* and *ACA2* complemented plants (*above*), and for *aca4aca11* and *aca1aca2aca7* mutant (*below*) plants compared against the corresponding model simulations (black bars). Letters indicate

788 significant differences (P<0.01). Note the highly significant slowing in g_s kinetics of the
789 mutant in the second and third steps to 1000 μbar CO_2.
790 (e-g) Cytosolic-free [Ca^{2+}] ([Ca^{2+}]$_i$) recorded from *aca4aca11* mutant guard cells of
791 Arabidopsis pre-loaded with the Ca^{2+}-sensitive fluorescent dye Fura-Red and challenged
792 with 1000 μbar CO_2. Images (e) and timecourse of measurements (f) for the guard cells of
793 three stomata from the same epidermal peel challenged with pCO_2 steps separated by 45-
794 min intervals. Images corresponding to the first and third steps pCO_2 steps are pseudo-color
795 coded for [Ca^{2+}]$_i$ (scale, *right*). The light-shaded structures correspond to chloroplasts and
796 were omitted from analysis. Image scale bar, 5 μm. Timecourse data (f) are means ±SE of
797 measurements from n≥6 points around the periphery of each guard cell pair. Note the rise in
798 [Ca^{2+}]$_i$ after 10 min is much reduced on the second and third steps to 1000 μbar CO_2 and its
799 recovery is delayed on returning to 400 μbar CO_2. Analysis of the timecourses (f) and
800 endpoints (g) for [Ca^{2+}]$_i$ recorded from n≥9 independent experiments show a suppression in
801 elevated [Ca^{2+}]$_i$ with successive pCO_2 steps. Time points are cross-referenced to the
802 experimental protocol (g, *above*) by the circled numbers. Small circles in (g) are individual
803 experimental data with means ±SE indicated by large circles and error bars. Filled and open
804 symbols are *aca4aca11* mutant and *ACA11*-complemented *aca4aca11* mutant guard cells,
805 respectively. Letters indicate significant differences (P<0.02). Similar results were obtained
806 for the *aca1aca2aca7* mutant and ACA2-complemented guard cells and are summarized in
807 Supplemental Figure S8.
808
809

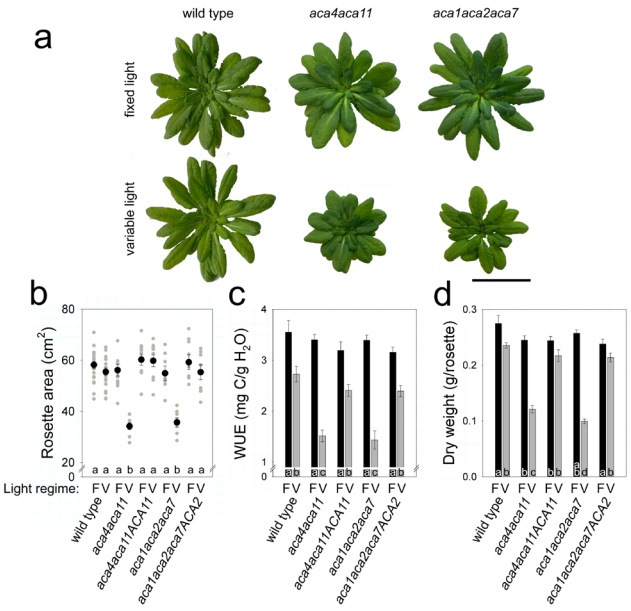

Figure 6. **Latency in stomatal kinetics affects long-term water use efficiency and plant growth.** (a,b) Representative wild-type, *aca4aca11*, and *aca1aca2aca7* mutant Arabidopsis plants (a) after 5 wk growth under fixed (F) and variable (V) light regimes (see Methods). Rosette areas (b) for all wild-type, *aca4aca11* and *aca1aca2aca7* mutant plants and the *ACA11* and *ACA2* complemented mutants, respectively, including the plants shown in (a). Small grey circles are individual plants; large filled circles are means ±SE for each set of plants (wild-type n=20 plants; mutant and complemented n=10 plants).
(c,d) Water use efficiency (WUE, c) and dry biomass (d) derived for the plants in (a,b). Supplemental Figure S6 includes the corresponding total Ca^{2+} content analysis.

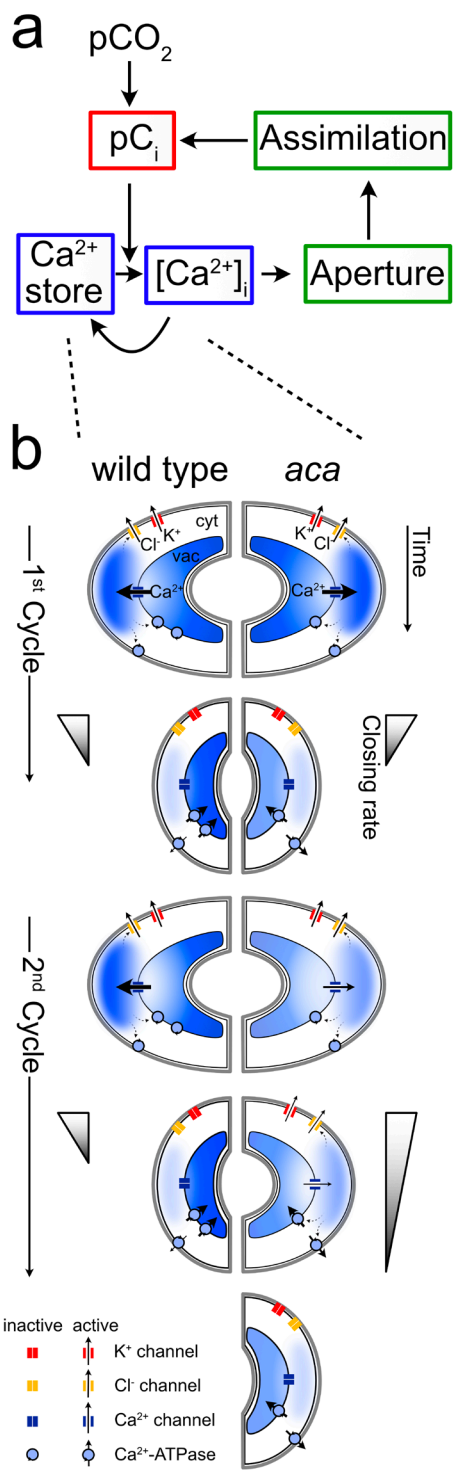

Figure 7. **A latent 'carbon memory' in stomatal responsiveness depends on guard cell endomembrane Ca^{2+} stores.** Schematic of the latency in stomatal responsiveness to light and CO_2 and its dependence on Ca^{2+} stores. (a) Cyclic network of connections between pC_i, $[Ca^{2+}]_I$, stomatal aperture, and photosynthetic assimilation. The latency, or 'carbon memory', in responsiveness arises from the delay in recovery of the Ca^{2+} stores following Ca^{2+} release and $[Ca^{2+}]_I$ elevations. (b) Temporal comparison of events as wild type (*left*) and the aca mutants (*right*) progress through two successive cycles (*top to bottom*) of elevated pC_i following an extended period of steady-state opening. For clarity, shown only are the Ca^{2+} relations (Ca^{2+} content indicated by blue shading intensity) with vacuolar Ca^{2+} cycling, the channels mediating K^+ and Cl^- efflux at the plasma membrane the Ca^{2+} channel at the tonoplast, and the Ca^{2+}-ATPases at the plasma membrane and tonoplast (*legend, bottom left*). Arrow thickness indicates ion transport rate and shaded triangles indicate stomatal closing rate.

With the first rise in pC_i, both wild-type and mutant stomata elevate cytosolic-free $[Ca^{2+}]$ ($[Ca^{2+}]_i$) drawing on full complements of stored Ca^{2+}. Resting $[Ca^{2+}]_i$ is recovered primarily through Ca^{2+} resequestration but, with the reduced tonoplast flux capacity in the *aca* stoma, a larger fraction of Ca^{2+} is proposed initially to be exported across the plasma membrane. Recovery of Ca^{2+} via entry across the plasma membrane (not shown) would normally refill the stores over longer times. With an early second rise in pC_i, however, the reduced store of Ca^{2+} impairs Ca^{2+} channel gating and release, thereby suppressing the rise in $[Ca^{2+}]_i$, slowing K^+ and Cl^- efflux and stomatal closure, as if retaining a 'carbon memory' reflected in an increased latency in response to the second rise in pC_i.

REFERENCES

1 Jezek, M. & Blatt, M. R. The Membrane Transport System of the Guard Cell and Its Integration for Stomatal Dynamics. *Plant Physiology* **174**, 487-519, doi:10.1104/pp.16.01949 (2017).

2 Lawson, T. & Blatt, M. R. Stomatal Size, Speed, and Responsiveness Impact on Photosynthesis and Water Use Efficiency. *Plant Physiology* **164**, 1556-1570 (2014).

3 Roelfsema, M. R. & Hedrich, R. Making sense out of Ca^{2+} signals: their role in regulating stomatal movements. *Plant Cell And Environment* **33**, 305-321 (2010).

4 Willmer, C. & Fricker, M. D. Vol. 2 1-375 (Chapman and Hall, London, 1996).

5 Buckley, T. N. & Mott, K. A. Dynamics of stomatal water relations during the humidity response: implications of two hypothetical mechanisms. *Plant Cell And Environment* **25**, 407-419 (2002).

6 Shope, J. C., Peak, D. & Mott, K. A. Stomatal responses to humidity in isolated epidermes. *Plant Cell And Environment* **31**, 1290-1298 (2008).

7 Ball, J. T., Woodrow, I. E. & Berry, J. A. in *Progress in Photosynthesis Research* Vol. 1 (ed J. Biggens) 221-224 (Martinus-Nijhoff, 1987).

8 Mott, K. A., Sibbernsen, E. D. & Shope, J. C. The role of the mesophyll in stomatal responses to light and CO 2 *Plant Cell And Environment* **31**, 1299-1306 (2008).

9 Papanatsiou, M. *et al.* Optogenetic manipulation of stomatal kinetics improves carbon assimilation and water use efficiency. *Science* **363**, 1456-1459 (2019).

10 Blatt, M. R. & Armstrong, F. K^+ channels of stomatal guard cells: abscisic acid-evoked control of the outward rectifier mediated by cytoplasmic pH. *Planta* **191**, 330-341 (1993).

11 Irving, H. R., Gehring, C. A. & Parish, R. W. Changes in cytosolic pH and calcium of guard cells precede stomatal movements. *Proceedings Of The National Academy Of Sciences Of The United States Of America* **89**, 1790-1794 (1992).

12 Webb, A. A. R., McAinsh, M. R., Mansfield, T. A. & Hetherington, A. M. Carbon dioxide induces increases in guard cell cytosolic free calcium. *Plant Journal* **9**, 297-304 (1996).

13 Assmann, S. M. & Jegla, T. Guard cell sensory systems: recent insights on stomatal responses to light, abscisic acid, and CO2. *Current Opinion in Plant Biology* **33**, 157-167, doi:10.1016/j.pbi.2016.07.003 (2016).

14 Zhang, J. *et al.* Insights into the Molecular Mechanisms of CO2-Mediated Regulation of Stomatal Movements. *Current Biology* **28**, R1356-R1363, doi:10.1016/j.cub.2018.10.015 (2018).

15 Brearley, J., Venis, M. A. & Blatt, M. R. The effect of elevated CO_2 concentrations on K^+ and anion channels of Vicia faba L. guard cells. *Planta* **203**, 145-154 (1997).
16 Wang, Y. *et al.* Unexpected Connections between Humidity and Ion Transport Discovered using a Model to Bridge Guard Cell-to-Leaf Scales. *Plant Cell* **29**, 2921-2139, doi:10.1105/tpc.17.00694 (2017).
17 Pilot, G. *et al.* Guard cell inward K + channel activity in Arabidopsis involves expression of the twin channel subunits KAT1 and KAT2. *Journal Of Biological Chemistry* **276**, 3215-3221 (2001).
18 Geiger, D. *et al.* Guard cell anion channel SLAC1 is regulated by CDPK protein kinases with distinct Ca^{2+} affinities. *Proceedings Of The National Academy Of Sciences Of The United States Of America* **107**, 8023-8028 (2010).
19 Brandt, B. *et al.* Reconstitution of abscisic acid activation of SLAC1 anion channel by CPK6 and OST1 kinases and branched ABI1 PP2C phosphatase action. *Proceedings of the National Academy of Sciences* **109**, 10593-10598, doi:10.1073/pnas.1116590109 (2012).
20 Wang, C. *et al.* Reconstitution of CO2 Regulation of SLAC1 Anion Channel and Function of CO2-Permeable PIP2;1 Aquaporin as CARBONIC ANHYDRASE4 Interactor. *Plant Cell* **28**, 568-582, doi:10.1105/tpc.15.00637 (2016).
21 Hills, A., Chen, Z. H., Amtmann, A., Blatt, M. R. & Lew, V. L. OnGuard, a Computational Platform for Quantitative Kinetic Modeling of Guard Cell Physiology. *Plant Physiology* **159**, 1026-1042 (2012).
22 Chen, Z. H. *et al.* Systems Dynamic Modeling of the Stomatal Guard Cell Predicts Emergent Behaviors in Transport, Signaling, and Volume Control. *Plant Physiology* **159**, 1235-1251 (2012).
23 Wang, Y. *et al.* Systems dynamic modelling of a guard cell Cl^- channel mutant uncovers an emergent homeostatic network regulating stomatal transpiration. *Plant Physiology* **160**, 1956-1972 (2012).
24 Jezek, M., Hills, A., Blatt, M. R. & Lew, V. L. A constraint-relaxation-recovery mechanism for stomatal dynamics. *Plant, Cell & Environment* **42**, 2399-2410, doi:10.1111/pce.13568 (2019).
25 Peak, D. & Mott, K. A. A new, vapour-phase mechanism for stomatal responses to humidity and temperature. *Plant Cell And Environment* **34**, 162-178 (2011).
26 Berry, J. A., Beerling, D. J. & Franks, P. J. Stomata: key players in the earth system, past and present. *Current Opinion In Plant Biology* **13**, 233-240 (2010).
27 Lawson, T., Simkin, A. J., Kelly, G. & Granot, D. Mesophyll photosynthesis and guard cell metabolism impacts on stomatal behaviour. *New Phytologist* **203**, 1064-1081, doi:10.1111/nph.12945 (2014).

28 Buckley, T. N. & Mott, K. A. Modelling stomatal conductance in response to environmental factors. *Plant Cell and Environment* **36**, 1691-1699, doi:10.1111/pce.12140 (2013).

29 Vialet-Chabrand, S. *et al.* Global Sensitivity Analysis of OnGuard Models Identifies Key Hubs for Transport Interaction in Stomatal Dynamics. *Plant Physiology* **174**, 680-688, doi:10.1104/pp.17.00170 (2017).

30 Roelfsema, M. R. G. & Hedrich, R. In the light of stomatal opening: new insights into 'the Watergate'. *New Phytologist* **167**, 665-691 (2005).

31 Kollist, H., Nuhkat, M. & Roelfsema, M. R. G. Closing gaps: linking elements that control stomatal movement. *New Phytologist* **203**, 44-62, doi:10.1111/nph.12832 (2014).

32 Hu, H. H. *et al.* Carbonic anhydrases are upstream regulators of CO_2 -controlled stomatal movements in guard cells. *Nature Cell Biology* **12**, 87-90 (2010).

33 Morison, J. I. L. & Jarvis, P. G. DIRECT AND INDIRECT EFFECTS OF LIGHT ON STOMATA .2. IN COMMELINA-COMMUNIS L. *Plant Cell and Environment* **6**, 103-109, doi:10.1111/j.1365-3040.1983.tb01882.x (1983).

34 Zhu, J., Talbott, L. D., Jin, X. & Zeiger, E. The stomatal response to CO2 is linked to changes in guard cell zeaxanthin. *Plant Cell and Environment* **21**, 813-820, doi:10.1046/j.1365-3040.1998.00323.x (1998).

35 Hiyama, A. *et al.* Blue light and CO2 signals converge to regulate light-induced stomatal opening. *Nature Communications* **8**, doi:10.1038/s41467-017-01237-5 (2017).

36 Medeiros, D. B. *et al.* Enhanced Photosynthesis and Growth in atquac1 Knockout Mutants Are Due to Altered Organic Acid Accumulation and an Increase in Both Stomatal and Mesophyll Conductance. *Plant Physiology* **170**, 86-101, doi:10.1104/pp.15.01053 (2016).

37 Merilo, E. *et al.* PYR/RCAR Receptors Contribute to Ozone-, Reduced Air Humidity-, Darkness-, and CO 2 -Induced Stomatal Regulation. *Plant Physiology* **162**, 1652-1668 (2013).

38 Tian, W. *et al.* A molecular pathway for CO_2 response in Arabidopsis guard cells. *Nature Communications* **6**, doi:10.1038/ncomms7057 (2015).

39 Grabov, A. & Blatt, M. R. A steep dependence of inward-rectifying potassium channels on cytosolic free calcium concentration increase evoked by hyperpolarization in guard cells. *Plant Physiology* **119**, 277-287 (1999).

40 Minguet-Parramona, C. *et al.* An Optimal Frequency in Ca^{2+} Oscillations for Stomatal Closure Is an Emergent Property of Ion Transport in Guard Cells. *Plant Physiology* **170**, 32-45, doi:10.1104/pp.15.01607 (2016).

41 Grabov, A. & Blatt, M. R. Membrane voltage initiates Ca^{2+} waves and potentiates Ca^{2+} increases with abscisic acid in stomatal guard cells. *Proceedings Of The National Academy Of Sciences Of The United States Of America* **95**, 4778-4783 (1998).

42 Blatt, M. R. Cellular signaling and volume control in stomatal movements in plants. *Annual Review Of Cell And Developmental Biology* **16**, 221-241 (2000).

43 Boursiac, Y. *et al.* Disruption of the Vacuolar Calcium-ATPases in Arabidopsis Results in the Activation of a Salicylic Acid-Dependent Programmed Cell Death Pathway. *Plant Physiology* **154**, 1158-1171, doi:10.1104/pp.110.159038 (2010).

44 Hwang, I., Sze, H. & Harper, J. F. A calcium-dependent protein kinase can inhibit a calmodulin- stimulated Ca 2+ pump (ACA2) located in the endoplasmic reticulum of Arabidopsis *Proceedings Of The National Academy Of Sciences Of The United States Of America* **97**, 6224-6229 (2000).

45 Conn, S. J. *et al.* Cell-Specific Vacuolar Calcium Storage Mediated by CAX1 Regulates Apoplastic Calcium Concentration, Gas Exchange, and Plant Productivity in Arabidopsis. *Plant Cell* **23**, 240-257 (2011).

46 Rahmati-Ishka, M. *et al.* Ca^{2+}-ATPases 1, 2, and 7 in the ER are important for Arabidopsis growth and pollen fitness. *Plant Physiology* **in press**, in press (2021).

47 Takemiya, A. *et al.* Phosphorylation of BLUS1 kinase by phototropins is a primary step in stomatal opening. *Nature Communications* **4**, doi:10.1038/ncomms3094 (2013).

48 Isner, J. C., Begum, A., Nuehse, T., Hetherington, A. M. & Maathuis, F. J. M. KIN7 Kinase Regulates the Vacuolar TPK1 K+ Channel during Stomatal Closure. *Current Biology* **28**, 466-472, doi:10.1016/j.cub.2017.12.046 (2018).

49 Ando, E. & Kinoshita, T. Red Light-Induced Phosphorylation of Plasma Membrane H+-ATPase in Stomatal Guard Cells. *Plant Physiology* **178**, 838-849, doi:10.1104/pp.18.00544 (2018).

50 Farquhar, G. D. & Sharkey, T. D. STOMATAL CONDUCTANCE AND PHOTOSYNTHESIS. *Annual Review of Plant Physiology and Plant Molecular Biology* **33**, 317-345, doi:10.1146/annurev.pp.33.060182.001533 (1982).

51 Endy, D. & Brent, R. Modelling cellular behaviour. *Nature* **409**, 391-395 (2001).

52 Xue, S. *et al.* Central functions of bicarbonate in S-type anion channel activation and OST1 protein kinase in CO2 signal transduction in guard cell. *Embo Journal* **30**, 1645-1658, doi:10.1038/emboj.2011.68 (2011).

53 Merlot, S. *et al.* Constitutive activation of a plasma membrane H^+ -ATPase prevents abscisic acid-mediated stomatal closure. *EMBO Journal* **26**, 3216-3226 (2007).

54 McAinsh, M. R., Webb, A. A. R., Taylor, J. E. & Hetherington, A. M. Stimulus-induced oscillations in guard cell cytosolic-free calcium. *Plant Cell* **7**, 1207-1219 (1995).
55 Garcia-Mata, C. *et al.* Nitric oxide regulates K^+ and Cl^- channels in guard cells through a subset of abscisic acid-evoked signaling pathways. *Proceedings Of The National Academy Of Sciences Of The United States Of America* **100**, 11116-11121 (2003).
56 Thor, K. & Peiter, E. Cytosolic calcium signals elicited by the pathogen-associated molecular pattern flg22 in stomatal guard cells are of an oscillatory nature. *New Phytologist* **204**, 873-881, doi:10.1111/nph.13064 (2014).
57 Resentini, F., Ruberti, C., Grenzi, M., Bonza, M. & Costa, A. The signatures of organellar calcium. *Plant Physiology* **186**, in press (2021).
58 Yang, H. M., Zhang, X. Y., Wang, G. X. & Zhang, J. H. Water channels are involved in stomatal oscillations encoded by parameter-specific cytosolic calcium oscillations. *Journal of Integrative Plant Biology* **48**, 790-799 (2006).
59 Kaiser, H. & Kappen, L. Stomatal oscillations at small apertures: indications for a fundamental insufficiency of stomatal feedback-control inherent in the stomatal turgor mechanism. *Journal Of Experimental Botany* **52**, 1303-1313 (2001).
60 Cowan, I. R. Oscillations in stomatal conductance and plant functioning associated with stomatal conductance - observations and a model. *Planta* **106**, 185-& (1972).
61 Lang, A. R. G., Klepper, B. & Cumming, M. J. Leaf water balance during oscillation of stomatal aperture. *Plant Physiology* **44**, 826-832 (1969).
62 Eckstein, J., Beyschlag, W., Mott, K. A. & Ryel, R. J. Changes in photon flux can induce stomatal patchiness. *Plant Cell and Environment* **19**, 1066-1074, doi:10.1111/j.1365-3040.1996.tb00213.x (1996).
63 Vialet-Chabrand, S. R. M. *et al.* Temporal Dynamics of Stomatal Behavior: Modeling and Implications for Photosynthesis and Water Use. *Plant Physiology* **174**, 603-613, doi:10.1104/pp.17.00125 (2017).
64 Yang, X. *et al.* A roadmap for research on crassulacean acid metabolism (CAM) to enhance sustainable food and bioenergy production in a hotter, drier world. *New Phytologist* **207**, 491-504, doi:10.1111/nph.13393 (2015).
65 Manzoni, S. *et al.* Hydraulic limits on maximum plant transpiration and the emergence of the safety-efficiency trade-off. *New Phytologist* **198**, 169-178 (2013).
66 Vico, G., Manzoni, S., Palmroth, S. & Katul, G. Effects of stomatal delays on the economics of leaf gas exchange under intermittent light regimes. *New Phytologist* **192**, 640-652 (2011).
67 Buckley, T. N. & Schymanski, S. J. Stomatal optimisation in relation to atmospheric CO2. *New Phytologist* **201**, 372-377, doi:10.1111/nph.12552 (2014).

68 Lin, Y.-S. *et al.* Optimal stomatal behaviour around the world. *Nature Climate Change* **5**, 459-464, doi:10.1038/nclimate2550 (2015).
69 Schymanski, S. J., Roderick, M. L., Sivapalan, M., Hutley, L. B. & Beringer, J. A canopy-scale test of the optimal water-use hypothesis. *Plant Cell and Environment* **31**, 97-111, doi:10.1111/j.1365-3040.2007.01740.x (2008).
70 Ball, M. C. & Farquhar, G. D. PHOTOSYNTHETIC AND STOMATAL RESPONSES OF 2 MANGROVE SPECIES, AEGICERAS-CORNICULATUM AND AVICENNIA-MARINA, TO LONG-TERM SALINITY AND HUMIDITY CONDITIONS. *Plant Physiology* **74**, 1-6, doi:10.1104/pp.74.1.1 (1984).
71 Pieruschka, R., Huber, G. & Berry, J. A. Control of transpiration by radiation. *Proceedings Of The National Academy Of Sciences Of The United States Of America* **107**, 13372-13377 (2010).
72 Damour, G., Simonneau, T., Cochard, H. & Urban, L. An overview of models of stomatal conductance at the leaf level. *Plant Cell and Environment* **33**, 1419-1438, doi:10.1111/j.1365-3040.2010.02181.x (2010).
73 Lavergne, A. *et al.* Observed and modelled historical trends in the water-use efficiency of plants and ecosystems. *Global Change Biology* **25**, 2242-2257, doi:10.1111/gcb.14634 (2019).
74 Keenan, T. F. *et al.* Increase in forest water-use efficiency as atmospheric carbon dioxide concentrations rise. *Nature* **499**, 324-+, doi:10.1038/nature12291 (2013).
75 Rasband, W. S. & Bright, D. S. NIH IMAGE - A public domain image-processing program for the Macintosh. *Microbeam Analysis* **4**, 137-149 (1995).
76 Alonso, J. M. *et al.* Genome-wide Insertional mutagenesis of Arabidopsis thaliana *Science* **301**, 653-657 (2003).
77 Kleinboelting, N., Huep, G., Kloetgen, A., Viehoever, P. & Weisshaar, B. GABI-Kat SimpleSearch: new features of the Arabidopsis thaliana T-DNA mutant database. *Nucleic Acids Research* **40**, D1211-D1215, doi:10.1093/nar/gkr1047 (2012).
78 McElver, J. *et al.* Insertional mutagenesis of genes required for seed development in Arabidopsis thaliana. *Genetics* **159**, 1751-1763 (2001).
79 Chen, Z. H., Hills, A., Lim, C. K. & Blatt, M. R. Dynamic regulation of guard cell anion channels by cytosolic free Ca^{2+} concentration and protein phosphorylation. *Plant Journal* **61**, 816-825 (2010).
80 Blatt, M. R. Electrical characteristics of stomatal guard cells: the contribution of ATP-dependent, "electrogenic" transport revealed by current-voltage and difference-current-voltage analysis. *Journal Of Membrane Biology* **98**, 257-274 (1987).
81 MacRobbie, E. A. C. & Lettau, J. Ion content and aperture in isolated guard cells of Commelina communis L. *Journal Of Membrane Biology* **53**, 199-205 (1980).

82 Squire, G. R. & Mansfield, T. A. SIMPLE METHOD OF ISOLATING STOMATA ON DETACHED EPIDERMIS BY LOW PH TREATMENT - OBSERVATIONS OF IMPORTANCE OF SUBSIDIARY CELLS. *New Phytologist* **71**, 1033-+, doi:10.1111/j.1469-8137.1972.tb01981.x (1972).

83 Kurebayashi, N., Harkins, A. B. & Baylor, S. M. Use Of Fura Red As An Intracellular Calcium Indicator In Frog Skeletal-Muscle Fibers. *Biophysical Journal* **64**, 1934-1960, doi:10.1016/s0006-3495(93)81564-9 (1993).

84 von Caemmerer, S. Steady-state models of photosynthesis. *Plant Cell and Environment* **36**, 1617-1630, doi:10.1111/pce.12098 (2013).

85 Ogren, E. & Evans, J. R. PHOTOSYNTHETIC LIGHT-RESPONSE CURVES .1. THE INFLUENCE OF CO2 PARTIAL-PRESSURE AND LEAF INVERSION. *Planta* **189**, 182-190, doi:10.1007/bf00195075 (1993).

86 Morison, J. I. L. *et al.* Lateral diffusion of CO_2 in leaves is not sufficient to support photosynthesis. *Plant Physiology* **139**, 254-266 (2005).

87 Parkhurst, D. F., Wong, S. C., Farquhar, G. D. & Cowan, I. R. GRADIENTS OF INTERCELLULAR CO2 LEVELS ACROSS THE LEAF MESOPHYLL. *Plant Physiology* **86**, 1032-1037, doi:10.1104/pp.86.4.1032 (1988).

88 Marquardt, D. An algorithm for least-squares estimation of nonlinear parameters. *J.Soc.Ind.Appl.Math.* **11**, 431-441 (1963).